Volume 17, Number 2, 2024. pp. 187-196

Jordan Journal of Physics

ARTICLE

Field Electron Emission from a Tungsten Cathode Coated with Silica

Ammar Alsoud[a,b], **Marwan S. Mousa**[c], **Adel M. Abuamr**[c], **Saleh H. Fawaeer**[a], **Kipkurui Ronoh**[a], **Ali F. AlQaisi**[c], **Karel Liedermann**[b], **Alexandr Knápek**[d], **M-Ali H. Al-Akhras**[e] and **Dinara Sobola**[a,b,c]

[a] *Central European Institute of Technology, Brno University of Technology, 612 00 Brno, Czech Republic.*

[b] *Department of Physics, Brno University of Technology Brno, 616 00 Brno, Czech Republic.*

[c] *Department of Physics, Mutah University, 61710 Al-Karak, Jordan.*

[d] *Institute of Scientific Instruments of the Czech Academy of Sciences, 612 64 Brno, Czech Republic.*

[e] *Department of Physics, Jordan University of Science and Technology, 22110 Irbid, Jordan.*

Doi: **https://doi.org/10.47011/17.2.6**

Received on: 15/02/2023; *Accepted on: 17/09/2023*

Abstract: The aim of this paper is to study the field electron emission of silicon dioxide-coated tungsten cathode. Tungsten tips of less than 100 nm radius were prepared by electrochemical etching. The size of silicon dioxide (silica) nanoparticles ranged from 3 to 15 nm. Field emission studies were conducted using a field emission microscope under high vacuum conditions. The images of the cathodes under investigation were taken using scanning electron microscopy. The results of the study of cathodes by energy-dispersive X-ray spectroscopy revealed tungsten as the dominant element with minimal silicon detected on the coated cathode surfaces. Murphy-Good plots were used to illustrate and analyze the current-voltage characteristics of the cathodes before and after coating. Moreover, patterns of electron emission both before and after the coating procedure were examined. The stability test of the emission current was performed on the composite cathode. The results indicate that the composite tungsten cathode performs better than the uncoated cathode, demonstrating increased emission current magnitude and enhanced stability of the emission current. The study presents silica nanoparticles as potential candidates for field emission sources coating across different applications.

Keywords: Field electron emission, Nanoparticles, Silica, Emission pattern, Stability test.

1. Introduction

In 1928, Fowler and Nordheim developed the first successful model for the cathode emission mechanism to analyze and understand its physics. Field electron emission (FE) is a process by which electrons are emitted from a material's surface due to an external electric field (typically about 3 V/nm) [1]. In 1956, Murphy and Good (MG) developed the "standard" theory of cold field electron emission (CFE) by using the Schottky-Nordheim (SN) barrier [2]. When the potential-energy barrier is sufficiently decreased, tunneling mostly occurs from electron states near the cathode Fermi level through the formation of a field emission electron beam [3, 4].

Corresponding Author: Ammar Al Soud **Email**: ammar.al.soud@vutbr.cz

An "electronically ideal" field emitter is one where the relationship between the measured current I_m and the measured voltage V_m is determined by the emission physics and the electrostatics of the system geometry alone. Many modern emitters are not electronically ideal [5]. The Murphy-Good equation shows the relationship between the emitted current I_m and the measured applied voltage V_m, which depends on the local work function ϕ of the material used, and the formal emission area for an SN barrier A_f^{SN}[4]:

$$I_m = A_f^{SN} a\phi^{-1}\zeta_C^{-2}V_m^2 \exp\left(-v_F b\phi^{\frac{3}{2}}\zeta_C V_m^{-1}\right) \quad (1)$$

Here, a and b are the first and second Fowler-Nordheim constants, ζ_C is the characteristic voltage conversion length, and v_F is a mathematical correction factor stated in the theory of the SN barrier.

There are several methods available for the analysis of the field emission current-voltage (*I-V*) characteristics. The most recent and precise way for assessing the results of the analysis is the MG plot [6]. MG plots have the form $\ln(I/V^{\kappa})$ vs V^{-1}, where κ is the Murphy-Good plot's pre-exponential factor. If only barrier effects are taken into account, then κ is given by [4] as

$$\kappa = 2 - \frac{\eta(\phi)}{6} \quad (2a)$$

where $\eta(\phi)$ is a scaling parameter given by [5]:

$$\eta(\phi) \cong 9.836239\ (\mathrm{eV}/\phi)^{1/2}. \quad (2b)$$

Generally, the MG equation can be applied to analyze field emission data when the material's local work function is well-defined. A theoretical Murphy-Good plot is described by Eq. (3) [4, 7]:

$$\ln\{\tfrac{I_m}{V_m^{\kappa}}\} = \ln\{A_f^{SN}\,\theta\,\exp\eta\ V_{mR}^{-\kappa}\} - \eta\,(V_{mR}/V_m), \quad (3)$$

where $\theta(\phi)$ and $\eta(\phi)$ are the scaling parameters, and V_{mR} is the reference measured voltage. For tungsten with ϕ = 4.5 eV, this equation is practically identical to a linear equation in field emission data, and the scaled field f_C [$=V_m/V_{mR}$] ranges from 0.15 to 0.45 [8]. For silica with ϕ = 5 eV, f_C is in the range between 0.14 and 0.43 [4]. Field emission data can be analyzed using the MG equation if the local work functions of the materials are adequately known.

Parameters extracted from the analysis process can be validated by means of the conventional field emission orthodoxy test [9]. These parameters can be summarized as extracted scaled field MG plot slope and the formal emission area following the measurement of the current-voltage characteristics. This quantitative test will validate the parameters obtained from the uncoated cathode under investigation and examine its state [8]. Therefore, before the development of the orthodoxy experiment, there were no appreciable modifications to the cathode's properties from a theoretical standpoint [4, 6].

Many previous studies have focused on field electron emission from composite cathodes, significantly contributing to the development of this technology. The emitter coating consists of a thin layer of insulating material characterized by low switch-on voltage, low switch-on current, high beam brightness, and the ability to sustain itself for many hours without appreciable decay [10, 11]. FE composite cathodes have many applications such as scanning electron microscopy [12], ultra-fast switching microwave amplifiers and generators [13], pressure sensors [14], and parallel electron beam lithography [15].

In recent years, extensive experimental research has focused on field emissions using various materials, particularly tungsten. Tungsten has several properties that make it the most popular material as an electron source in field emission studies such as hardness, high density, high melting point (3414°C), chemical stability, and simple preparation method of nano-cathode by using electrochemical etching as a cathode production technique [16–18].

Moreover, recent studies have explored coated electron sources such as tungsten-epoxy [17, 18], tungsten/polystyrene [17], tungsten/magnesium oxide nanoparticles, and carbon fibers/polystyrene [19]. According to the available data, the electron emission process has significantly improved, including a higher emission current value, a lower threshold voltage, a longer emitter lifetime, a brighter emission image, and a greater condensed electron beam.

This study examines the outcomes from two different electron sources: the tungsten-silica composite cathode and the uncoated tungsten tip. The findings are expected to provide valuable

insights applicable to the characterization parameters of cathodes [17, 20].

2. Experimental Methods

High-purity polycrystalline tungsten samples (99.995%) with a diameter of 0.3 mm and a length of 1 cm were used to prepare the field emission nanotips by means of an Armin-m etching/coating device. This device, developed at the Institute of Scientific Instruments of the Czech Academy of Sciences, exists in both manual and fully automated versions [21]. This instrument can provide field emission nanotips with an apex radius of less than 100 nm using the drop-off electrochemical etching method. The parts of this device and the electro-etching technique have been covered in previous studies [16, 21]. After the preparation of the samples, any residual hydroxide solution on the surface of the tips was removed by cleaning in an ethanol ultrasonic bath for 20 minutes.

Silica, commonly known as silicon dioxide (SiO_2), is a naturally occurring substance composed of silicon (Si) and oxygen (O_2). SiO_2 nanoparticles with very high purity (99.95%) and particle sizes ranging from 3 to 15 nm were obtained from Sigma-Aldrich Company, USA. Silica has high melting and boiling points of 1610 °C and 2230 °C, respectively [22]. However, due to the zero polarity of its molecule and the fact that it is insoluble in both water and acids, the compound is non-reactive. Moreover, silica has high dielectric strength, making it suitable for use as an insulator and semiconductor [23, 24]. The work function of SiO_2 is reported to be 5 eV [25], corresponding to $\kappa = 1.266850$.

The coating solution was prepared by mixing 1 mg SiO_2 with 3 ml of ethanol. The solution was then placed in an ultrasonic bath for 10 minutes to ensure homogeneity [22]. Subsequently, the solution was heated for 20 minutes at a temperature of 80 ℃ Subsequently, the alcohol, resulting in a thick SiO_2 coating solution ready to use [23, 24]. The coating process was performed using the manual version of the Armin-m device and involved two main steps of controlled tip dipping. Initially, the uncoated tip was dipped slowly and perpendicularly into the coating solution. This step was repeated to produce thicker coating layers [10, 16]. The second step involved heating the coated tips in an oven (Naberthem D-2804 Lilienthal / Bremen, Germany) for 20 minutes at 80 ℃ to expel the solvent (alcohol) from the tip surface.

A scanning electron microscope (SEM) was used to obtain micrographs of each cathode both before and after coating. This was done in order to check that the silica coating layer was uniformly distributed and to measure its thickness before beginning the field emission experiment. Electron beams with an accelerating voltage of 5 kV were directed onto the FE nanotips, and SEM images were acquired from secondary electrons at a magnification of 1340X. The radius of each cathode tip was determined using SEM software for measurement. The elemental composition of the cathode was determined using Energy Dispersive X-ray spectroscopy (EDS) (Oxford Instruments, UK), which was attached to the scanning electron microscope (MIRA3-XMU, Tescan) and operated within an energy range of 20 keV.

The prepared samples were characterized using a field electron microscope (FEM) to examine field electron emission from the nano-cathode. The FEM system was locally built at Mutah University, Jordan, using pumps and gauges from Edwards (UK). In this system, the emitter was mounted at a distance of 1 cm and operated under low pressures (up to 10-7 mbar). This high vacuum is necessary to decrease the back bombardment of ionized gas molecules onto the cathode tip in order to protect it from being damaged. Emission images were visualized on a phosphorus indium tin oxide (ITO) coated screen and recorded directly using a Nikon DX digital camera mounted at a distance of 35 cm from the screen. The samples were linked to a high voltage power supply with a range of 0 - 6000 V, while the phosphorous screen was grounded through a precision picoammeter Keithely 405 to measure the total emission current. Measurements of the I-V characteristics from a cathode took about two hours and included three cycles, each lasting 40 minutes. A stability test was conducted over a duration of 60 minutes.

3. Results and Discussion

This work presents the results of tungsten cathodes before and after coating with a thin layer of SiO_2. The results are discussed in the following sections.

3.1. SEM Micrographs

The SEM micrographs for both uncoated and coated cathodes are shown in Figs. 1(A) and 1(B), respectively. Figure 1(A) depicts the uncoated cathode after cleaning to ensure no NaOH layer remains on the surface of the cathode before coating. Figure 1(B) shows the cathode after being coated with a thin layer of silica nanoparticles. The radius of the clean tip is approximately 90 nm, while the thickness of the coating layer is approximately 110 nm. Subtracting the radius of the uncoated tip (90 nm) from that of the coated tip (200 nm), as measured from the SEM micrographs, establishes the thickness of the coating layer at approximately 110 nm.

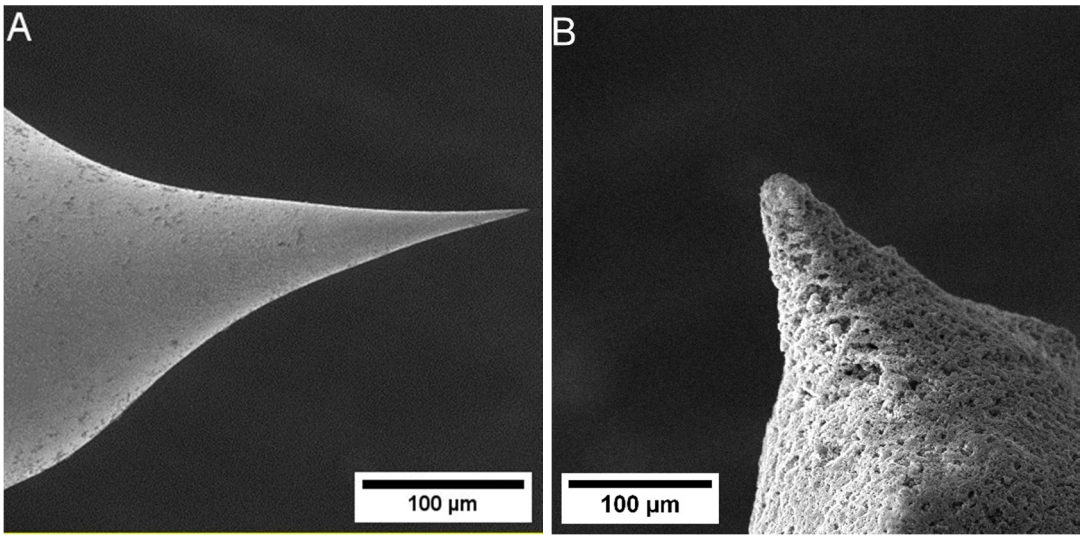

FIG. 1. SEM images of the (A) uncoated cathode, and (B) coated cathode.

3.2 Scanning Electron Microscopy–Energy Dispersive Spectrum (SEM-EDS)

Scanning electron microscopy–energy dispersive spectrum (SEM-EDS) was used to determine the composition and purity of the field emission cathode after the etching process. Figure 2 shows the SEM-EDS analysis spectra for the coated cathode. Two measurements of the SEM-EDS spectrum were made: one away from the tip (near the narrowing) (spectrum 1, uncoated area), and one on the coated surface (spectrum 2). Figure 2(A) (spectrum 1) results show that even though tungsten is dominant, there are detectable contaminants such as carbon (C) and oxygen (O). The carbon contaminant may originate from the SEM chamber or the environment where it gets adsorbed onto the cathode surfaces. Oxygen could originate from the air and/or from the silica coating, probably due to decomposition [26].

From spectrum 1, sodium or nickel elements from the etching process were not detected. Moreover, the tungsten showed a high concentration in the chemical composition, indicating effective sample cleaning using ethanol and current measurements after numerous full cycles.

In spectrum 2, a high concentration of silicon was observed, with an overlap of the Si and W lines.

3.3 Emission Characteristics Obtained from the Uncoated Cathode

The I-V characteristics and MG plot of the uncoated cathodes for the third cycle are shown in Figs. 3(A) and 3(B). At 700 V, the emission begins with a current of 3 nA. The voltage that was being applied was subsequently raised to 2000 V. During the cycle of decreasing voltage, the voltage is reduced until the current drops to zero at a threshold voltage of 800 V.

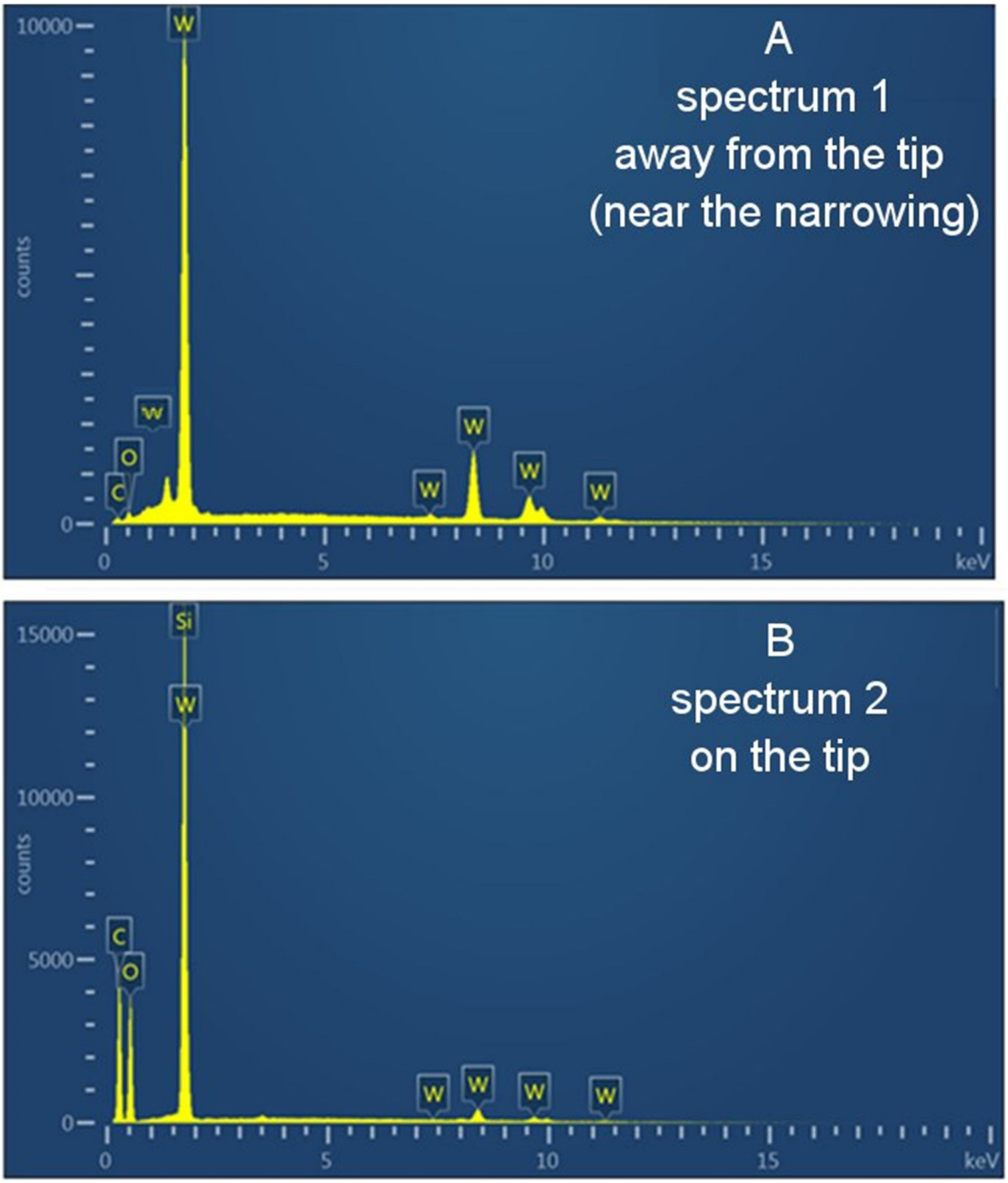

FIG. 2. The SEM-EDS analysis spectrum for a sample coated with silica. (A) Spectrum 1 is in the region away from the tip (near the narrowing). (B) Spectrum 2 is the EDS at the tip.

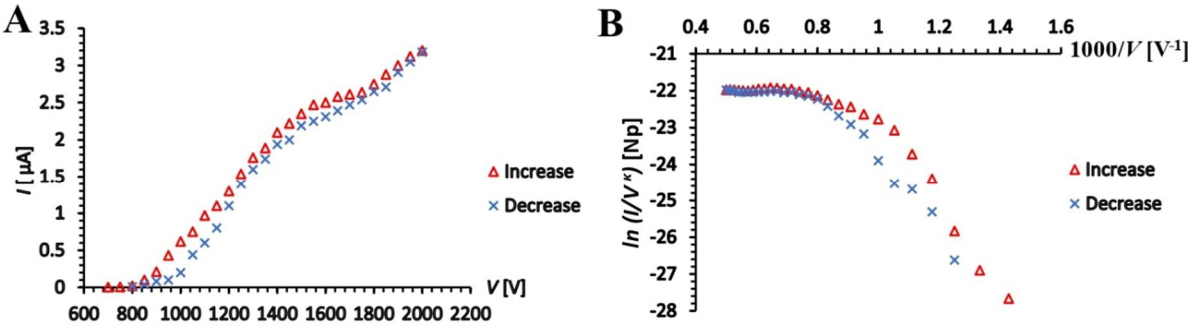

FIG. 3. (A) The current-voltage characteristics, (B) the Murphy-Good analysis plots of the uncoated FE cathode.

It is well known [9] that, for an electronically ideal FE system, an MG plot from a clean, well-defined tungsten emitter forms a nearly straight line across the entire range of operating voltages. It is also possible for FE systems to be effectively ideal only over a certain part of their operating range (usually the low-voltage part). Several researchers have predicted this nonlinear behavior and investigated it theoretically and experimentally [25, 27].

To check whether the low-voltage regime in our measurements exhibits "ideal" system behavior, the field emission orthodoxy test was applied to this part of the characteristics [3, 28]. For the uncoated samples, the test voltage ranged from 700 to 1000 V, with the decreasing part ranging from 800 to 1050 V. The field electron emission data were analyzed using a web tool to obtain exact results for the orthodoxy test [28]. The samples passed the test. Therefore, it was possible to utilize this part of our results as the baseline cathode for the experiment before proceeding with the addition of coating layers. In Table 1, the results of the field emission orthodoxy test are displayed.

TABLE 1. Field emission orthodoxy test results for the uncoated cathode using MG analysis.

Cycle part	Voltage range [V]	Extracted scaled field emission values	Slope [Np V]	Formal Emission Area Value (Af)[m^2]	Test result
Increase	700 – 1000	0.27 – 0.36	-12.21	1.710e-20	pass
Decrease	1050 –850	0.32 – 0.36	-11.59	2.371e-21	pass

According to the summary of the results from a field emission experiment shown in Table 1, the uncoated cathode condition did not appear to change appreciably [4, 6]. This includes parameters such as the emission area, slope, and the extracted scaled field emission and voltage conversion length of the cathode used.

Since the uncoated sample passed the orthodoxy test, we can now proceed to study the emission characteristics of the coated sample.

3.4 Emission Characteristics Obtained from the Composite Cathode

Figures 4(A) and 4(B) present the $I_m(V_m)$ characteristics and MG analysis of the voltage-decreasing part following the observation of the switch-on phenomenon [10]. Starting from zero volts, the applied voltage was gradually increased until the appearance of a high electrical current (in microamperes). This event is referred to as the switch-on phenomenon [11]. The switch-on phenomenon was observed at V_{sw} = 700 V, where the saturated emission current was I_{SW} = 3.2 μA. After stabilizing the current, the current in the saturation region was very small (700-680 V). The applied voltage was gradually decreased, and the lowest value of current at which emission could be seen was I_m = 0.1 μA at V_m = 500 V.

The $I_m(V_m)$ characteristics for the full cycle and its MG analysis are presented in Figs. 5(A) and 5(B), respectively. The emission process started at V_m = 500 V and I_m = 0.1 μA, and the voltage was slowly raised to V_m = 2000 V and I_{sat} = 6.51 μA. After that, the voltage was reduced slowly until no emission electrons could be observed at (V_m = 700 V and I_m = 0.1 μA).

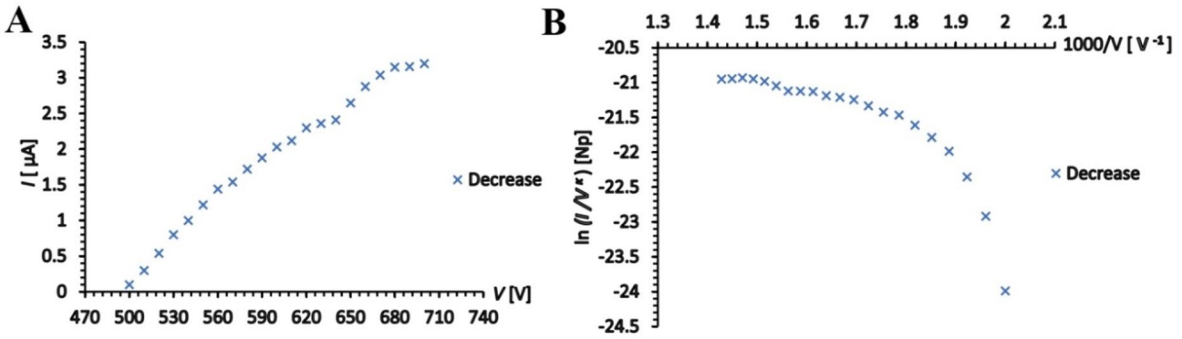

FIG. 4. (A) The current-voltage characteristics and (B) The Murphy-Good analysis plot of the coated FE cathode from the initial voltage decrease phase.

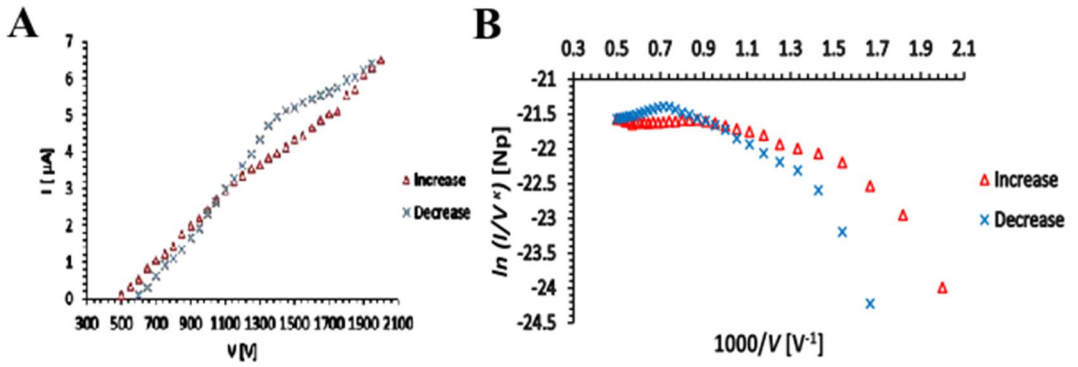

FIG. 5. (A) The current-voltage characteristics; and (B) The Murphy-Good analysis plots from the composite cathode's complete cycle.

The apex radius of the uncoated cathode and the thickness of the SiO_2 layer appear to significantly influence the emission current from the composite cathode. Comparing the current-voltage characteristics of coated and uncoated cathode samples reveals that the efficiency of the composite cathode is more than that of the uncoated cathode. We can contrast the results obtained for the two cases at an applied voltage value of 1500 V. The current value from the uncoated cathode was 2.2 μA, while the value from the composite cathode was 5.4 μA. This demonstrates that the composite cathode's emission current value is 2.5 times higher than that of the uncoated cathode.

It is noteworthy that the switch-on phenomenon observed when several hundred volts were applied to the tip exhibited a lower switch-on current compared to previous studies when other types of coating materials were used [10, 11, 16–18]. The reason for this is probably that the SiO_2 layer has a small electron affinity (0.6–0.8 eV) [29], which results in weak charge storage capability in the silicon oxide layer owing to its low dielectric constant. Also, the emission current through SiO_2 was found to be nearly independent of polarity. Although the bonds in SiO_2 are polar due to the higher electronegativity of oxygen compared to silicon, the linear arrangement of these bonds in opposite directions cancels out their dipoles. As a result, the net dipole moment is zero [30, 31].

3.5 Emission Patterns

The emission patterns obtained from the uncoated cathode are shown in Figs. 6(A)-6(C). Similarly, the emission patterns obtained from composite cathodes are shown in Figs. 6 (D)-6(F).

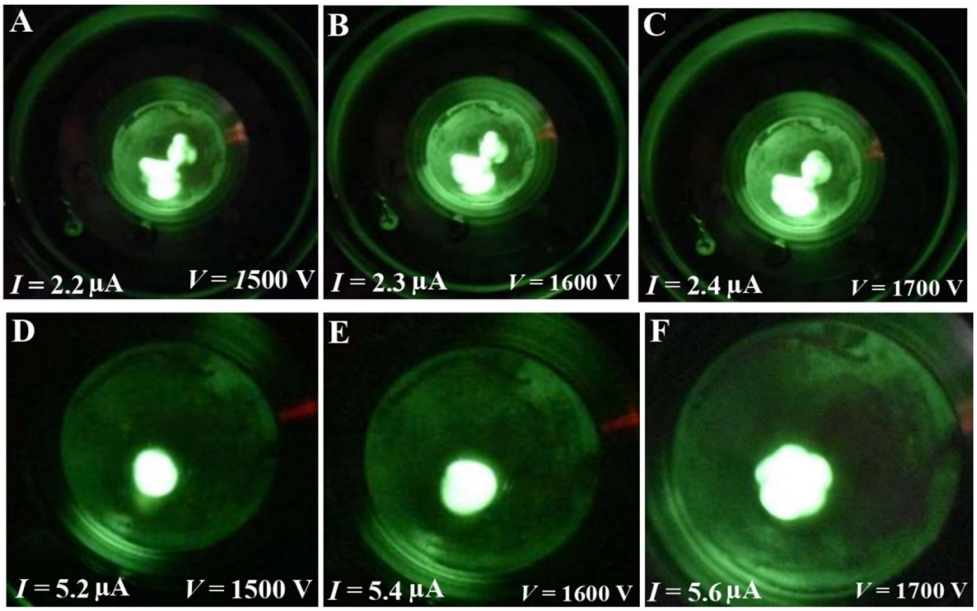

FIG. 6. (A) – (C) Emission patterns and current distribution images for the uncoated cathode. (D) – (F) Emission patterns and current distribution images for the composite cathode.

The "uncoated" emission patterns differ significantly from the well-established (e.g. [29]) patterns associated with a clean tungsten emitter. This shows that our "uncoated" emitters are not "clean" but likely coated with a layer of adsorbates, probably originating from the fabrication process or the vacuum environment. This phenomenon may be typical for most or all uncoated emitters prepared under "industrial working conditions", so our results may have relevance in this context. Similar patterns of emission have been observed in previous research [16, 19].

Characterizing basic aspects of electron emission, such as solid angle, apex source size, and electron beam brightness, allows for a comprehensive assessment of the electron emission source. Brightness (β) measures the spot size and the amount of emission current concentrated within a particular solid angle ($d\Omega$), where ($d\Omega$) is a function of the apex source radius, the brightest part of the emitted electron beam, and the current densities [32]. Comparisons are made based on the apex radius rather than the emission area (A). The concept of "apex radius" is well defined as the area where electrons are generated. It is possible to get the apex radius from a scanning electron microscope (SEM) image [25]. High brightness means that the electrons are emitted at a narrow solid angle, with a large amount of emission current at low voltage, where the emission current (I) can be deduced from the relation [27]:

$$I = \beta A d\Omega \quad (4)$$

In Figs. 6(A)-6(C), the emission current of the uncoated cathode is 2.2 µA, 2.3 µA, and 2.4 µA, respectively. In Figs. 6(D)-6(F), the emission current of the composite cathode is 5.2 µA, 5.4 µA, and 5.6 µA, respectively. Therefore, the emission current of the coated cathode more than doubled compared to that of the uncoated cathode. Also, the emission area in Figs. 6(D)-6(F) area is approximately half the original area shown in Figs. 6(A)-6(C). By comparing these data and using Eq. (4), it can be concluded that the brightness from the composite cathodes is at least four times greater than that of the uncoated cathode. This result has important technological implications for the development of new cathodes as electron sources. After applying s sufficiently high electric field to the composite cathodes (10^9 V m^{-1}) [11], electrons tunnel through the coating nanoparticle layer and get emitted into the vacuum onto the phosphorus screen. Based on previous work, the FEM emission current pattern for the uncoated cathode primarily consists of multiple bright spots. The pattern of the emission current for the composite cathode consists of a single light spot at the point where the emitted electrons impact the phosphor screen [11], [19].

Images in Fig. 6 show a comparison of the current value, emission pattern, and emission area of three voltage values: 1500 V, 1600 V, and 1700 V for both the uncoated cathode and the composite cathode. From the comparison results in Fig. 6, three main points can be made. First, the emission current of the composite cathode is higher than the emission current of the uncoated cathode. Second, the emission pattern of the composite cathode consists of a single spot, while the emission pattern of the uncoated cathode consists of multiple spots and is irregular. Third, the emission pattern of the composite cathode is brighter than the emission pattern of the uncoated cathode.

3.6 Stability Test

The field emission stability test of the composite cathode, as observed on a phosphorescent screen, is shown in Fig. 7. The stability of the composite cathode was monitored at a current of about 5.2 µA, under an applied voltage of 1500 V. The emission current has relatively long-term stability, with the structural pattern of the composite emitters being tested for 60 minutes. Emission pattern images were taken at a fixed time frequency of 15 min. The current values recorded during that period are represented in Fig. 7.

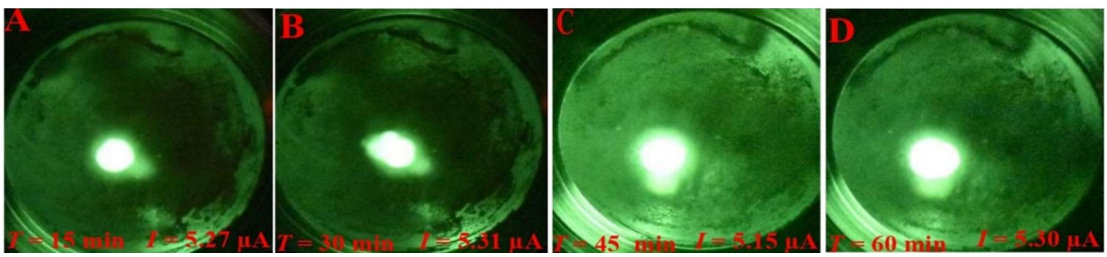

FIG. 7. Field emission stability test of the composite cathode for 60 minutes at 1500V.

Fig. 7 shows the stability of current values over time. This stability provides the coating material with an additional benefit, as it acts as a protective layer against bombardment from ionized gases, which could otherwise destroy the cathode or alter its chemical makeup.

4. Acknowledgements

CzechNanoLab project LM2023051 funded by MEYS CR is gratefully acknowledged for the financial support of the measurements and sample fabrication at CEITEC Nano Research Infrastructure. The authors would like to thank the support of the internal mobility grant of CEITEC BUT based on the memorandum of understanding between the University of Science and Technology and Brno University of Technology. We also acknowledge the Czech Academy of Sciences (RVO: 68081731) for providing the etching equipment and laboratory infrastructure. Moreover, the authors would like to acknowledge the support of the Deanship of Scientific Research of Mutah University through research projects #452/2021, 441/2021, and 442/2021.

5. Conclusions

In this study, a tungsten FE cathode tip was coated with silica, and its performance was investigated using SEM, EDS, and FEM. SEM analysis confirmed the presence of a silica thin layer on the tungsten tip, while EDX showed that W was the dominant element, with Si appearing on the coated tip. From FEM analysis, it was established that coating the tungsten cathode with a thin layer of silica improved some of the characteristics of the field electron emission process. The coating procedure resulted in higher current values and lower voltage switching. The study demonstrated that the field emission patterns for the tungsten-silica composite cathode were brighter and more concentrated than those of the uncoated tungsten cathode. Moreover, an increase in the field emission stability was observed in the coated tips.

This study established that, in general, using silica nanoparticles as a coating material improves emission current and stability, making it a potential candidate for coating field emission electron sources. Further studies will be undertaken to establish the effects of different specific sizes of silica nanoparticles on the field electron emission process. Additionally, research on a mixture of silica with epoxy as a coating material will be undertaken.

References

[1] Fowler, R.H. and Nordheim, L., Proc. R. Soc. Lond. A, 119 (1928) 173.

[2] Murphy, E.L. and Good, R.H., Phys. Rev., 102 (1956) 1464.

[3] Forbes, R.G., J. Vac. Sci. Technol. B, 26 (2008) 788.

[4] Allaham, M.M., Forbes, R.G., Knápek, A., Sobola, D., Burda, D., Sedlák, P. and Mousa, M.S., Mater. Today Commun., 31 (2022) 103654.

[5] Forbes, R.G., Proc. R. Soc. Lond. A, 469 (2013) 2158.

[6] Madanat, M., Al Share, M., Allaham, M.M. and Mousa, M.S., J. Vac. Sci. Technol. B, 39 (2021) 024001.

[7] Forbes, R.G., R. Soc. Open Sci., 6 (2019) 190912.

[8] Kyritsakis A. and Xanthakis, J.P., Proc. R. Soc. Lond., 471 (2015) 20140811.

[9] Forbes, R.G., J. Vac. Sci. Technol. B, 41 (2023) 028501.

[10] Mousa, M.S. and Al Share, M., Ultramicroscopy, 79 (1999) 195.

[11] Latham, R.V. and Mousa, M.S., J. Phys. D: Appl. Phys., 19 (1986) 699.

[12] Spindt, C.A., Holland, C.E., Brodie, I., Mooney, J.B. and Westerberg, E.R., IEEE Trans. Electron Devices, 36 (1989) 225.

[13] Feinerman, A.D., Crewe, D.A., Perng, D.C., Shoaf, S.E. and Crewe, A.V., J. Vac. Sci. Technol. A, 10 (1992) 611.

[14] Busta, H.H., J. Vac. Sci. Technol. B, 12 (1994) 689.

[15] Mancusi, J.E., Joines, W.T., McGuire, W.T., Temple, D., Vellenga, D.G. and Yadon, L., IEEE Trans. Electron Devices, 41 (1994).

[16] Al Soud, A., Knápek, A. and Mousa, M.S., Jordan J. Phys., 13 (2020) 191.

[17] Alabth, M., Shatnawi, M.T.M., Allaham, M.M., Burda, D. and Mousa, M.S., Ultramicroscopy, 244 (2023) 113643.

[18] Al Soud, A., Al Buqain, R.N. and Mousa, M.S., Jordan J. Phys., 13 (2020) 253.

[19] Fawaeer, S.H., Shatnawi, M.T.M., Allaham, M.M. and Mousa, M.S., Adv. Mater. and Process. Tech., 8 (2022) 2652.

[20] Zhou, Y. and Zhang, P.P., Phys. Rev., 2 (4) (2020) 043439.

[21] Knápek, A., Sýkora, J., Chlumská, J. and Sobola, D., Microelectron. Eng., 173 (2017) 42.

[22] Al Soud, A., Daradkeh, S., Knápek, A., Liedermann, K., Holcman, V. and Sobola, D., EEICT, 29 (2023) 253.

[23] Nekrashevich, S.S. and Gritsenko, V.A., Phys. Solid State, 56 (2014) 207.

[24] Schneider, P.M. and Fowler, W.B., Phys. Rev. Lett., 36 (8) (1976) 425.

[25] Madanat, M.A., Al-Tabbakh, A.A., Alsa'eed, M., Al-Dmour, H. and Mousa, M.S., Ultramicroscopy, 234 (2022) 113479.

[26] Ronoh, K., Fawaeer, S.H., Holcman, V., Knápek, A. and Sobola, D., Vacuum, 215 (2023) 112345

[27] Mousa, M.S. and Abuamr, A.M., Jordan J. Phys., 16 (2) (2023) 247.

[28] Allaham, M.M., Forbes, R.G., Knápek, A. and Mousa, M.S., "Field Emission Analysis Software", https://fieldemissionanalysis.weebly.com. accessed June 11, 2021

[29] Gomer, R., "Field Emission and Field Ionization", (Harvard Univ. Press, Cambridge, Mass,, 1961), p. 34.

[30] Wang, Q., Chen, G. and Alghamdi, A.S., IEEE, 2010 (2010) 4.

[31] Lu, Y.X., Lin, C.T., Tsai, M.H. and Lin, K.C., Micromachines, 13 (4) (2022) 509.

[32] Lee, H.R., Kim, D.W., Rodiansyah, A., Cho, B., Lim, J. and Park, K.C., Nanomaterials, 11 (8) (2021) 1918.